Earthquake Geotechnical Engineering for Protection and Development of Environment and Constructions – Silvestri & Moraci (Eds)
© 2019 Associazione Geotecnica Italiana, Rome, Italy, ISBN 978-0-367-14328-2

Numerical analysis of liquefaction countermeasure method by hexagonal grid form soil improvement using jet grouting method

Y. Isobe & M. Sekino
Geoscience Research Laboratory, Co., Ltd., Tokyo, Japan

J. Takeuchi, T. Oonishi & M. Nakajima
Nittoc Construction, Co., Ltd, Tokyo, Japan

ABSTRACT: The grid form soil improvement is one of the countermeasure construction methods to reduce liquefaction by restraining shear deformation of sandy ground during earthquake. A ground improvement method for restraining liquefaction has been newly developed. That is to construct hexagonal grid form soil improvements in the ground using the jet grouting method. Dynamic centrifuge model tests were carried out, and the effect of the newly developed construction method was verified. Numerical analysis by the three-dimensional dynamic finite element method was performed, and the deformation restraint effect of the proposed method was verified. The undrained cyclic triaxial test was also conducted to determine the parameters of the sand for numerical analysis. In the numerical analysis, the same condition as the centrifuge model test was set and ground motions were input from the centrifuge model test. It was confirmed that both centrifuge model test and numerical analysis have effect of liquefaction countermeasure.

1 INTRODUCTION

1.1 *Purpose of research*

The grid-like ground improvement is a countermeasure method to suppress the liquefaction by suppressing the shear deformation of the sand plate at the time of the earthquake so far. Dynamic FEM analysis of the lattice-shaped ground improvement cement mixtures as a countermeasure against liquefaction was carried out and the behavior at the time of a large earthquake was investigated (Namikawa et al. 2007). It has been confirmed that even when the improved body partially breaks, the required performance of the lattice-shaped improved ground of liquefaction prevention is satisfied. However, if it is a quadrilateral type, stress concentration may occur at the corner portion, which may increase the burden on the improved body. Therefore, the authors tried to use a high-pressure injection stirring method to replace a number of hexagonal grid-like ground improvement. Also, the distributions of shear stresses and strains in liquefiable soil deposits treated with deep soil mixing (DSM) grids are investigated using three-dimensional linear elastic finite-element analyses of unit cells (Nguyen et al. 2013). Although it is studied by three-dimensional analysis, it is limited to elasticity analysis rather than elasto-plastic analysis. Considering this kind of past investigations, we are working on the development of a new soil improvement method that creates and suppresses liquefaction. Numerical analysis can reproduce experimental results and aims to further reflect it in the design.

1.2 *Outline of numerical analysis*

Three-dimensional dynamic effective stress analysis by FEM was carried out for numerical analysis in which cyclic elasto-plastic constitutive model (Oka 1982, Oka et al. 1999). A liquefaction

analysis program LIQCA3D (2015 open version) which can perform consolidation analysis due to dissipation of excess pore water pressure was used (Oka et al. 2003, Oka et al. 2004, Oka et al. 2005). Numerical analysis code to solve the governing equation of the coupling problem of soil skeleton and pore water pressure based on solid dynamics. This coupled problem is derived from Biot's theory dealing with a saturated porous material composed of two phases, a solid phase and a liquid phase. Various formulations are made in Biot's equation by taking unknowns and approximating methods, but LIQCA uses u-p formulation with unknown as the displacement u of the solid phase and the pore water pressure p of the liquid phase (Oka et al. 1994). For the discretization of the governing equations, the finite element method is used for the spatial discretization of the force equilibrium, and the spatial discretization of the term of the continuous pore water pressure is a finite difference extended to the orthogonal lattice finite volume method is used. In addition, the Newmark-β method which is the implicit solution method is used for time discretization, and Rayleigh attenuation is used for attenuation.

The following assumptions are assumed for formulation.

1. Small strain
2. The porosity, the density of the liquid phase (pore water), the gradient of the hydraulic conductivity to the space are sufficiently small
3. The relative acceleration of the liquid phase with respect to the solid phase is sufficiently smaller than the acceleration of the solid phase
4. Soil particles are incompressible
5. Ignore temperature changes

1.3 FLOW OF NUMERICAL ANALYSIS

The flow of liquefaction analysis is shown in Figure 1.

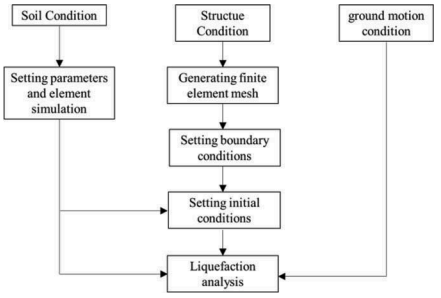

Figure 1. Flowchart of numerical analysis by LIQCA3D

2 OUTLINE OF DYNAMIC CENTRIFUGE MODEL TESTS

2.1 *Model ground*

The experiment was carried out with a similarity rate of 1/40 (centrifugal gravitational field 40 g) using a shear soil bath having a width of 700 mm, a depth of 270mm, and a height of 460 mm as shown in Figure 2. The model ground was made with the Toyoura-sand layer equivalent to 10 m as liquefiable soil layer which relative density is 60 % and the compacted soil layer equivalent to 2 m underneath the Toyoura-sand layer as non-liquefiable soil layer which relative density is 90 %. In planar view, the central part with the hexagonal grid form soil improvements was positioned as the liquefaction countermeasure ground, and the other areas were classified as no improved ground. The groundwater level was set to 1 m depth below ground level.

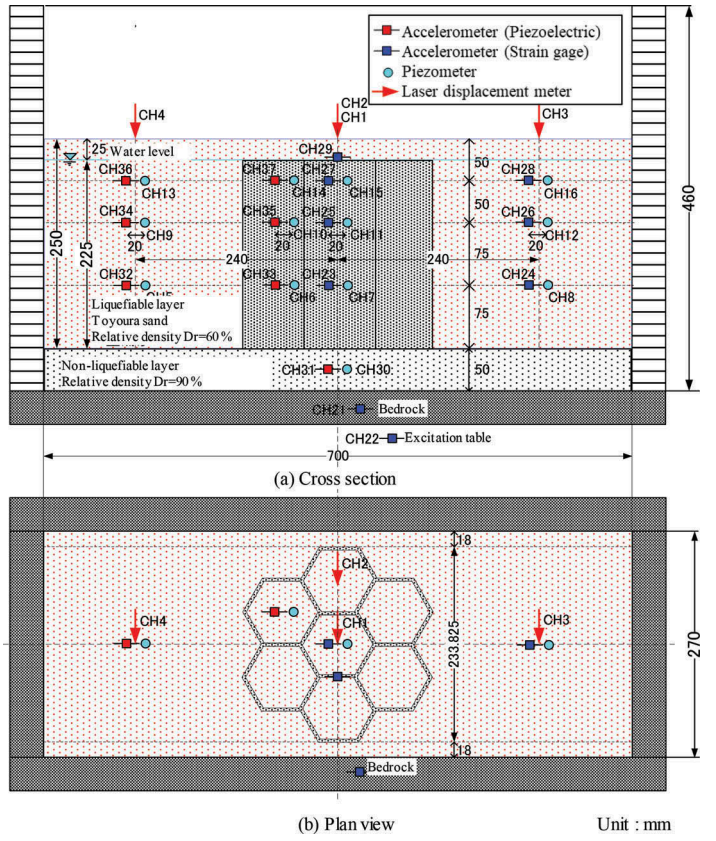

Figure 2. Outline of model tests

2.2 *Hexagonal grid form model*

The model was made of acrylic resin, and as shown in the Figure 3, seven hexagonal molds each having a side of 45 mm and a wall thickness of 4 mm viewed from the plane were arranged. The upper end of the model was aligned with the groundwater level, the lower end was aligned with the border of non-liquefiable layer, and it was installed in the center. As an installation procedure of hexagonal grid form model, after preparing the non-liquefiable layer by the compaction method to have a density of Dr = 90%, a hexagonal grid form model is placed on the non-liquefiable layer. Then, a liquefiable layer with Dr = 60% was produced by the air falling method.

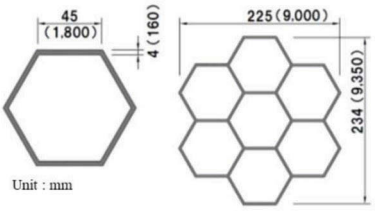

Figure 3. Outline of hexagonal grid form model

2.3 *Measurement items and configuration*

The measurement items are horizontal acceleration, excess pore water pressure and vertical displacement of the ground surface, and the configuration of each measuring instrument is shown in the Figure 2. In the liquefaction layer, we installed the accelerometer and the pore water pressure measurements in the improved area and in the non-improved area at three depths (equivalent to 2 m depth, 4 m depth, and 7 m depth) respectively. In addition, in order to measure the vertical displacement distribution of the ground surface, measurements were made at intervals of 1 cm using a laser displacement sensor.

2.4 *Excitation condition*

Excitation is generated from the excitation table and accelerometer CH22 is installed. In the excitation, three sine waves of 1.5 Hz were subjected to 20 waves, and the target acceleration obtained with CH21 at the bedrock not at the excitation table was carried out in three stages of 100 gal, 150 gal and 200 gal. At the end of each excitation, after confirming the dissipation of the excess pore water pressure, the next stage of excitation is carried out.

3 NUMERICAL ANALYSIS CONDITIONS

3.1 *Basic analysis conditons*

The analysis conditions are shown in Table 1. The cyclic elasto-plastic model was applied to the liquefaction layer, a modified Ramberg - Osgood model was applied to the non-liquefaction layer, and linear elastic model was applied to hexagonal grid form soil improvement. In the analysis, initial self-weight analysis, seismic response analysis, consolidation analysis was performed in order.

3.2 *Element simulation*

The material parameters of the liquefaction layer (Toyoura sand relative density Dr=60%) were identified from preliminary indoor soil test results, and the deformation characteristics were fitted with cyclic undrained triaxial test and dynamic deformation test results by element simulation value was used as shown in Figure 4. Table 2 shows parameter lists set by element simulation.

3.3 *Analysis model*

A finite element mesh is created considering a similarity rate of 40 times as centrifuge model test. The mesh size of the finite element in the vertical direction was 1 m high as shown in Figure 5.

Table 1. Analysis conditions

Item	Detail
Version	LIQCA3D15 (2015)
Soil	Liquefiable layer : cyclic elasto-plastic model Non-liqeufiable layer : modified Ramberg - Osgood model
Improvement	linear elastic model
Rayleigh damping	α_0=0.0, α_1=0.002
Newmark-β	β=0.3025, γ=0.6
Time interval	dt=0.005
Analysis phase	1. Initial self-weight analysis 2. Seismic response analysis 3. Consolidation analysis

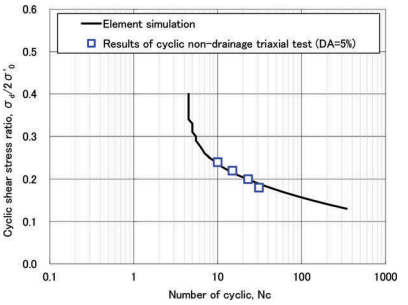

Figure 4. Fitting results of element simulation

Table 2. Parameters of cyclic elasto-plastic model

Density	ρ_t (t/m^3)	1.96
Initial void ratio	e_0	0.740
Permeability	k /γ_w	1.22E-05
Compression index	λ	0.0066
Swelling index	κ	0.00066
Initial shear modulus ratio	G_0/σ'_m	1007
Failure stress ratio	M^*_m	0.909
Phase transformation stress ratio	M^*_f	1.204
Hardening parameter	B^*_0	3500
Hardening parameter	B^*_1	35
Hardening parameter	C_f	0
Reference strain parameter	γ^{P*}_{ref}	0.0040
Reference strain parameter	γ^{E*}_{ref}	0.0200
Dilatancy parameter	D^*_0	1.0
Dilatancy parameter	n	5.0
Over consolidation ratio	OCR^*	1.2
Control parameter of anisotropy	C_d	2000
Bulk modulus	K_f(kN/m^2)	2.00E+06

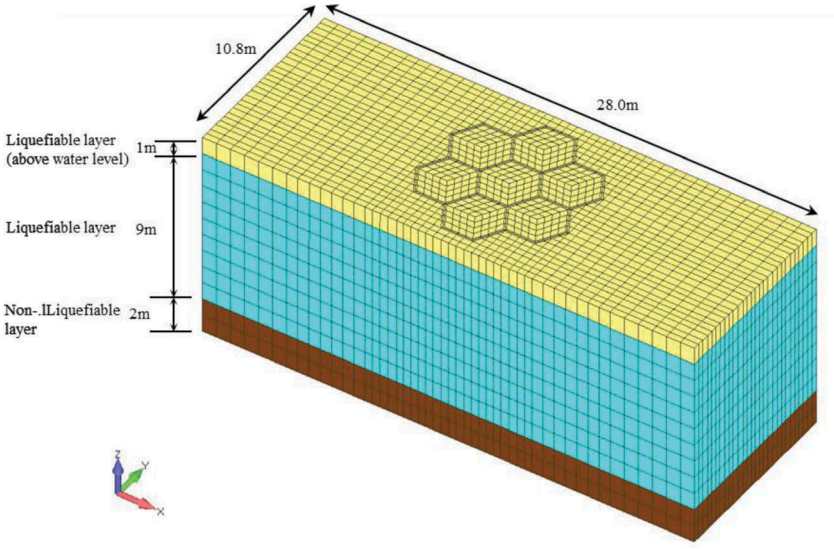

Figure 5. Finite element mesh

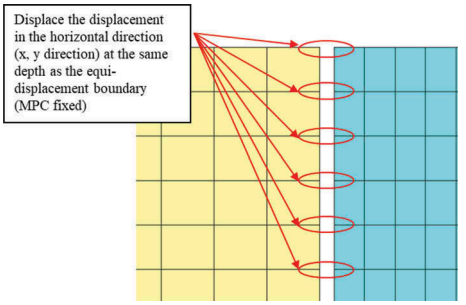

Figure 6. Setting discontinuity of ground and improvement

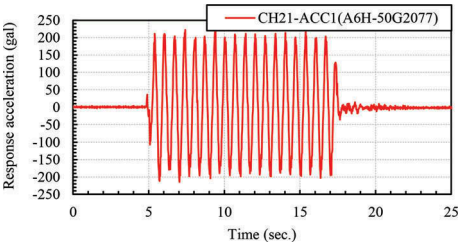

Figure 7. Input motion acceleration

3.4 *Boundary condition and excitation condition*

For the boundary condition of the seismic response analysis, a repetition boundary is set which constrains all nodes that are at the same height on the side of the analysis area at equal displacement. For the input seismic motion, we input the acceleration obtained at the base position of the centrifuge loaded model experiment apparatus. Analysis was conducted under the conditions targeting 200 gal at the bedrock in the experiment and compared with the experiment. The discontinuities of the ground and improvement is shown in Figure 6. The response acceleration at the bedrock obtained at the CH22 in the experiment as shown in Figure 2 was directly input for analysis as shown in Figure 7.

4 RESULTS

4.1 *Results of excess pore water pressure ratio*

The excess pore water pressure for each depth was compared at the position of the no-measure part (output 1), the grid central part (output 2) and the outer lattice inside (output 3) shown in Figure 8. Figure 9 shows the time historical comparison (actual scale) of the excess pore water pressure of the experimental results and analysis results. The measurement points indicated in Figure 9 are multiplied by the similarity rate to express the position compared with the experiment. Although the analytical result tends to show a slightly larger value than the experimental result at each position, the rising tendency of the excess pore water pressure is roughly in agreement and it can be said that the experiment result can be reproduced.

4.2 *Results of vertical displacement of ground level*

A comparison (actual scale) of the vertical displacement distribution of the ground surface is shown in Figure 10. In the experimental results, the settlement amount of the non-countermeasure part was large, and it was 12 cm or more, but in the central grid part and the outer

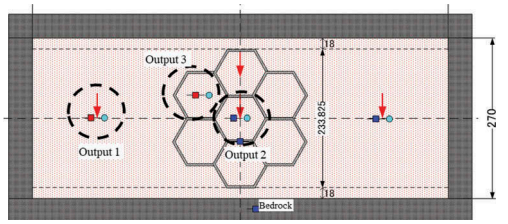

Figure 8. Output positions

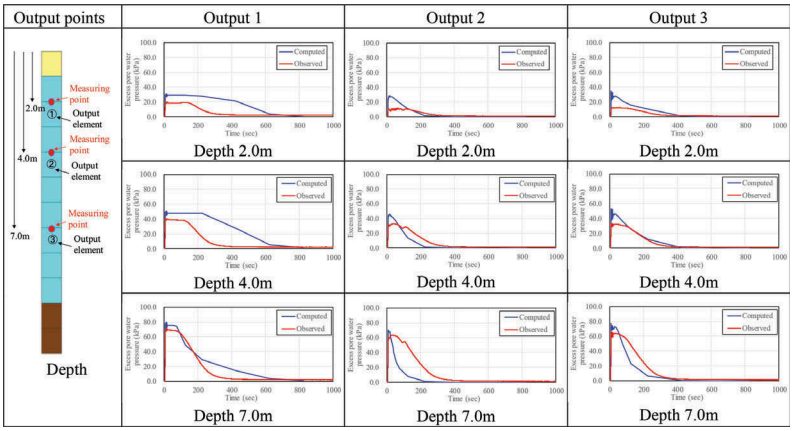

Figure 9. Time history results of excess pore water pressure at each depth

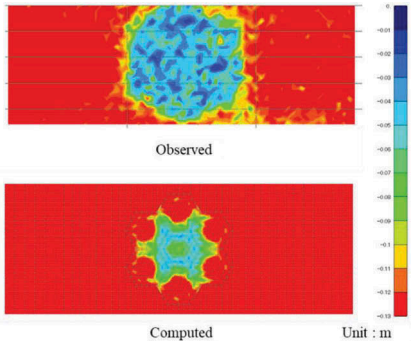

Figure 10. Vertical displacement distribution of the ground surface

grid part, the settlement amount was only about 2 to 4 cm and the sinking suppression effect of the hexagonal grid form improvement appeared greatly. On the other hand, in the analysis results, although the appearance of the improvement exhibiting the sinking suppression effect was observed, the settlement amount inside the outer lattice was larger than in the central part of the lattice, and the settlement amount of 10 to 12 cm was recorded. In the non-countermeasure area, as shown in Figure 11, the settlement amount of the hexagonal grid form soil improvement was the largest and the settlement amount was 20 cm or more at the maximum, about twice the experimental result. Settlement of ground surface is small around the center of the improved area where the rise of excess pore water pressure is small, and the excess pore water pressure increases greatly, and the settlement is also large in the free field of the unmodified part.

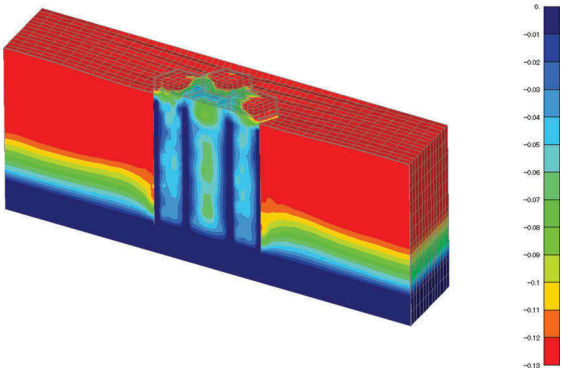

Figure 11. Vertical displacement distribution result by analysis (section cut view)

5 CONCLUSIONS

Experimental results and analysis results generally agreed with the rising tendency and maximum value of excess pore water pressure, and reproducibility was confirmed. In comparison with the amount of vertical displacement of the ground surface, the effect of suppressing the settling of hexagonal grid form soil improvements obtained in the centrifugal force model experiment was also confirmed in the reproducible analysis. However, in the interior of the lattice and in the non-countermeasure area, the amount of settlement of the analytical result was larger than the experimental result, and the sinking amount at the maximum was doubled. The liquefaction inhibiting effect of the hexagonal grid form soil improvements can be almost reproduced by three-dimensional effective stress analysis (LIQCA3D). As future works, it is necessary to quantitatively evaluate the liquefaction suppression effect by verifying the reproducibility on a two-dimensional model and analyzing it under a model close to an actual condition (ground condition and input ground motion).

REFERENCES

Namikawa, F., Koseki, J., and Suzuki, Y. 2007. Finite element analysis of lattice-shaped ground improvement by cement-mixing for liquefaction mitigation, *Soils and Foundation*: 47(3), 559–576.

Nguyen, T.V., Rayamajhi, D., Boulanger, R., and Ashford, S. A. 2013. Design of DSM Grids for Liquefaction Remediation, *Journal of Geotechnical and Geoenvironmental Engineering*: 139(11), 1923–1933.

Oka, F. 1982. Constitutive equations for granular materials in cyclic loading, *Proceedings of IUTAM Conference on Deformation and Failure Materials of Granular Materials*: 297–306. Delft

Oka, F., Yashima, A., Shibata, T., Kato, M., and Uzuoka, R. 1994. FEM-FDM coupled liquefaction analysis of a porous soil using an elasto-plastic model, *Applied Scientific Research*: 52, 209–245.

Oka, F., Yashima, A., Tateishi, A., Taguchi, Y. and Yamashita, S. 1999. A cyclic elasto-plastic constitutive model for sand considering a plastic-strain dependence of the shear modulus, *Geotechnique*: 49(5), 661–680.

Oka, F., Kodaka, T., Takyu, T., Yamazaki, N. and Ohno, Y. 2003. Deformation and strength characteristics ofimproved sand by a grouting materials and its application to liquefaction analysis of man made island, *Proc. XIII ECSMGE, I. Vanicek et al. Eds, CGtS, Prague*: 1, 861–866. Prague, Czech Republic

Oka, F., Furuya, K. and Uzuoka, R. 2004. Numerical simulation of cyclic behavior of dense sand using a cyclic elasto-plastic model, *Proceedings of Cyclic Behavior of Soils and Liquefaction Phenomena,Triantafyllidis (ed.)*: 85–90. Bochum

Oka, F., Furuya, K. and Uzuoka, R. 2005. Computational modeling of large deformations and the failure of geomaterials, *Proceedings of 16thICSMGE*: 1, 95–122.